International Journal of Heat and Technology
Vol. 42, No. 5, October, 2024, pp. 1794-1804
Journal homepage: http://iieta.org/journals/ijht

Energy-Exergy Analyzing of a Solar-Driven CCHP System Based on the First and Second Laws of Thermodynamics

Faeza Mahdi Hadi

Electrical Engineering Technical College, Middle Technical University, Baghdad 10001, Iraq

Corresponding Author Email: faeza@mtu.edu.iq

https://doi.org/10.18280/ijht.420534

Received: 9 August 2024
Revised: 2 October 2024
Accepted: 17 October 2023
Available online: 31 October 2024

Keywords:
energy analysis, CCHP, CAES, solar energy, ORC, refrigeration cycle

ABSTRACT

In this study, a solar-driven combined cooling-heating and power system is proposed to achieve higher energy efficiency. Influences of compression ratio and direct normal irradiance are reported to evaluate the impact of design parameters. A compressed air energy system technology is utilized in the solar-driven Brayton cycle to run it in the peak consumption time, and a Rankine cycle is employed as an axillary cycle for more power generation. Results prove that the proposed system provides 11.75 MW pure power besides 3.2 MW heating and 6.8 MW cooling loads and it is able to run 5 hr in compressor deactivated mode passing peak consumption hours. Overall energy efficiency of the proposed system is estimated by more than 55% considering solar inlet beams energy, and 89% ignoring solar tower energy loss. The most exergy destructor component of the proposed system is solar heat absorber by 72% of general system destructed exergy.

1. INTRODUCTION

Due to the environmental issues posed by fossil energy sources, reducing the effects of using these resources is one of the main priorities in energy planning today [1]. In this context, in addition to striving for maximum energy savings, the most important concern is to replace these energy resources with renewable ones [2]. Consequently, the use of fuel cell [3], wave [4], wind [5], and solar [6] energies attained substantial attention. Furthermore, wasted heat recovery is another promising approach to save the energy resources [7]. Running the combination of cooling, heat and power systems together, which is commonly named as Combined Cooling, Heating and Power (CCHP) systems [8], is considered as one of the technological suggestions to achieve this aim. However, the noticeable role of other-recently-flourished methods in energy sector, such as Artificial Intelligence (AI) [9], could not be neglected.

Solar energy as a green energy resource, is also employing noticeably for CCHP systems [10]. Sun beams will be trapped using solar tower [11] or solar concentrator [12], then the trapped heat will be transferred to the working fluid of power generator cycle. Indeed, Samiee and Aghdam [13] employed photovoltaic panels to direct electricity conversion in their CCHP which is proposed for cruise ship. They asserted that using hybrid energy resource, the proposed system produced 457.25 kW electricity. The solar driven CCHP system integrated with ammonia driven molten carbonate fuel cell, purposed by Lu et al. [14], shows 57.85% energy efficiency and 60.22%, exergy efficiency. They asserted that, the novel technique they used for heat absorption, enhanced solar power generation by 1.27%. Therefore, the novel system has a higher productivity and economic performance. A hydrogen production sub-system is added to the solar driven CCHP system investigated by Assareh et al. [15], to achieve 90% hydrogen production efficiency. The system cost is reported by \$514188.21 per year in case of optimum condition. To achieve sustainable and efficient poly-generation system, Liu et al. [16] investigated a solar assisted CCHP system thermodynamically. During this study, energy and exergy efficiencies are reported by 57.5% and 36.6% under design condition, respectively. Indeed, the carbon emission of investigated system is reported by 0.071 to 0.075 t/GJ.

CCHPs benefit a main power generation part which could be run by a Brayton [17], Rankine [18] or 4-stroke combustion [19] cycle. Therefore, the range of heat sources, wasted heat recovery sub-cycles, and performance improver sub-devices are widely extended [20]. A Brayton cycle is employed as the main power generation part of the solar driven poly-generation system investigated by Georgousis et al. [21]. They optimized the operating condition using multi-objective optimization approach and asserted that the payback period of their system is around 6.4 years while the total efficiency is 55%. They also reported that the exergy efficiency of the studied system could be enhanced up to 23.63% using additional Organic Rankine Cycle (ORC). Using Brayton cycle as the main power section, Zhang et al. [22] reported the Coefficient Of Performance (COP) for their CCHP system by 188.1%. Indeed, Rankine cycle is utilized as the main power generation section in a CCHP system investigated by Cao et al. [23]. Due to the high temperature exhaust flow from common Brayton cycle it is possible to run a Rankine cycle [24], supercritical CO_2 Brayton cycle [25], or ORC [26] as the wasted-heat recovery sub-section. Employing ORC in this case has advantages like, being energetically efficient and environmentally friendly besides enabling investment-savings [27].

Compressed Air Energy Storage (CAES) technology is known as the performance optimizer and enhancer of thermodynamic power cycles [28] as well as CCHP systems [29]. Mohammadi et al. [30] achieved 2.56 kW cooling load, 33.67 kW electricity and 1.82 ton/day hot water with 53.94% trip energy efficiency employing CAES coupled with wind turbine. Arabkoohsar et al. [31] accomplished 30.6, 2.5 and 14.4% exergy efficiencies of cooling, power and heat productions using their suggested configuration of CAES. Yang et al. [32] improved the energy efficiency of the studied CCHP by 1.015% with employing CAES technology and solar energy. Su et al. [33] also reported 77.8 and 3.3% electricity and natural gas saving ratios improvement using synthetic utilization of solar and biogas energy in their studied CCHP. Eisavi et al. [34] stated that the cooling and heating load of CCHP could be raised up to 48.5 and 20.5% employing solar energy.

Looking more detail in investigated literature, it can be asserted that there are lots of efforts all around the world to produce and optimize the renewable electricity using Braytone cycle and the technologies applied on it to enhance the performance shown in Figure 1. However, this approach needs to be improved constantly. The combination of studied approaches and technologies can be considered as one of the possible way to achieve this goal, so in this work, a novel solar-driven CCHP system using the combination of reviewed technologies is proposed for improving the energy efficiency. Then the influence of design parameters on system energy and exergy performance is evaluated in the parametric study to achieve optimal performance. Indeed, such a parametric study could bring the dataset for further AI-based optimization study.

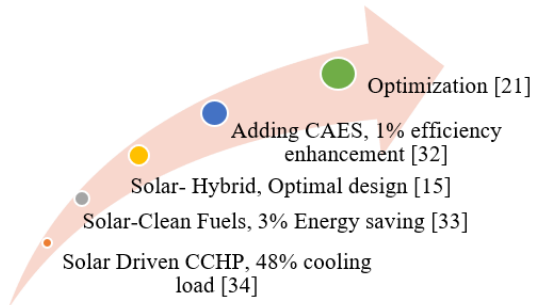

Figure 1. Solar driven CCHP trend line

2. SYSTEM DESCRIPTION

The schematic diagram of the proposed CCHP cycle is shown in Figure 2. It contains five sub-sections, namely; Brayton, Rankine, ORC, Refrigeration, and Heating systems which will be described at the following.

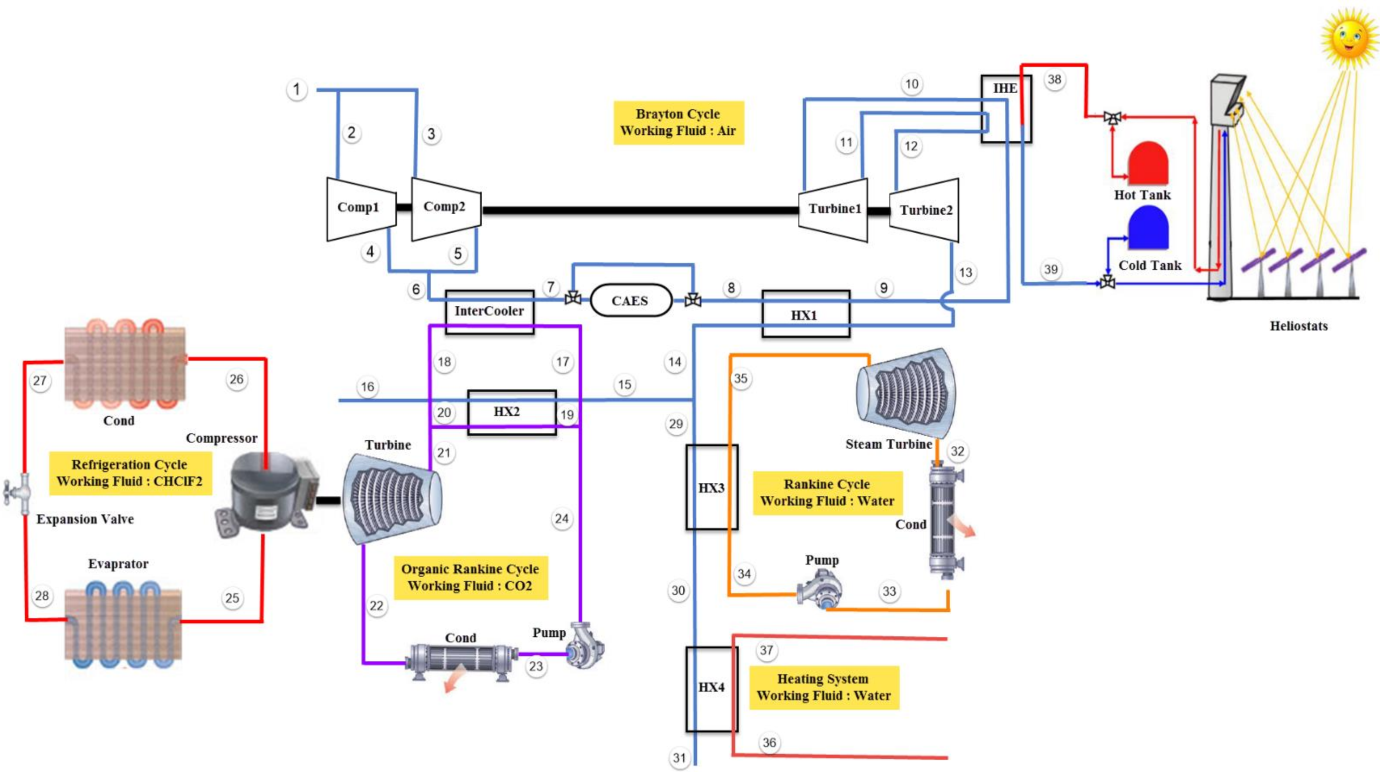

Figure 2. The schematic diagram of the proposed CCHP system

Fresh air is compressed up to 750 kPa by two parallel flow compressors (to provide demanded mass flow rate) with identical shafts in the Brayton cycle. Then its temperature is reduced near to the ambient in designed intercooler, and the waste heat is used to run an ORC driven refrigerator cycle. Cooled high pressure air then, is saved in the cavern to run the proposed system in peak consumption hours using compressors deactivation mode. Such a high pressure air then, is preheated through heat exchanger, and its temperature is increased up to 1025 K in the Intermediate Heat Exchanger (IHE) from solar tower. High energy air then, runs the turbines in two stages after reheating. The exhaust air is divided into the two parts, running Rankine and organic Rankine cycles, after cavern exhaust air preheating. The rest of the air energy is employed to provide the demanded hot water with the temperature of 373.1 K in the Heating System (HS). Used solar system configuration is adopted from reference [35], and the thermal storage tank is added to provide the demanded heat in the times the sun beams not receives sufficiently. The receiver, IHE, is located above the tower with 68.1 m^2 aperture area and the reflective area of each heliostat is considered as 121.4 m^2. The Rankine cycle is operated between 65 and 3000 kPa. The out power of steam turbine is directly converted to the electricity and added to the main Brayton cycle power output. Designed refrigeration cycle runs using the power provided by an ORC. This ORC works between 7000 and 15000 kPa. Although the high pressure line is above the critical pressure of CO_2, the condenser is still working under the critical pressure, and the high pressure working fluid is provided by a pump. So, this cycle is still categorized as the Rankine cycle. Using a simple one-stage compression refrigeration cycle beside the power provided by the ORC, the demanded cooling load is supplied. Considered working fluid is R22 ($CHClF_2$) which works between 263 and 308 K.

The main configuration parameters are adopted from the previous studies, however to enhance the overall performance besides tackle the operational limitations (e.g.: the streamlines temperatures at heat exchangers), setting or optimizing some of the operational parameters is necessary. For example, the designed temperatures of evaporator (T_{25}) and condenser (T_{27}) outflows are selected based on having optimum COP in the refrigeration cycle shown in Figure 3. Furthermore, inlet heat from solar system is divided between two steams (9-10 and 11-12) at IHE, considering the turbine inlet temperature (T_{10} and T_{12}) limitation. The variations of IHE outflows temperatures based on the heat division rate are shown in Figure 4.

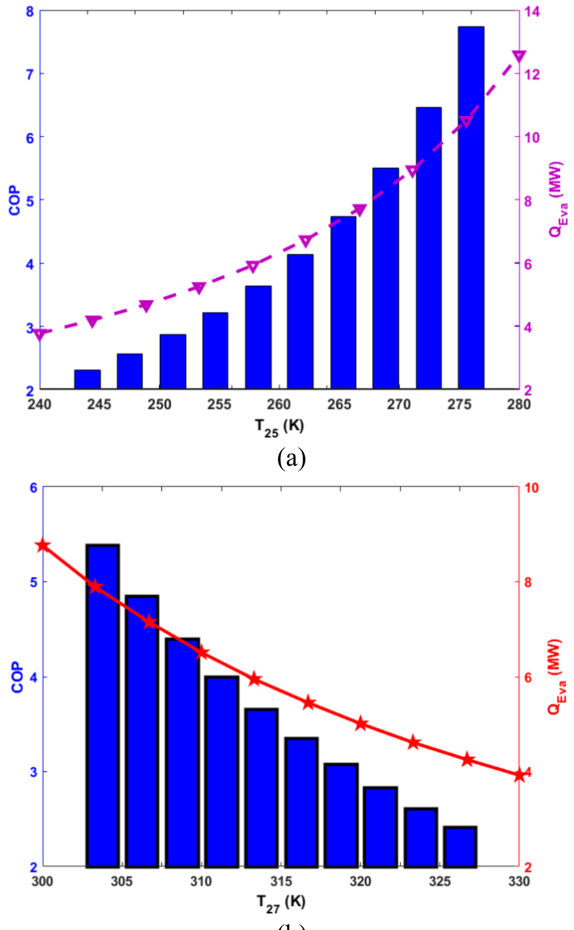

Figure 3. COP and cooling load variations with a) evaporator, b) condenser operating temperatures

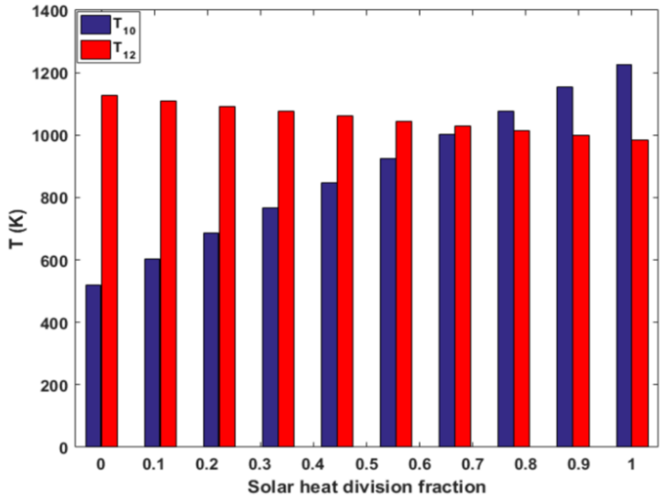

Figure 4. IHE outflows temperatures variations with solar heat division fraction

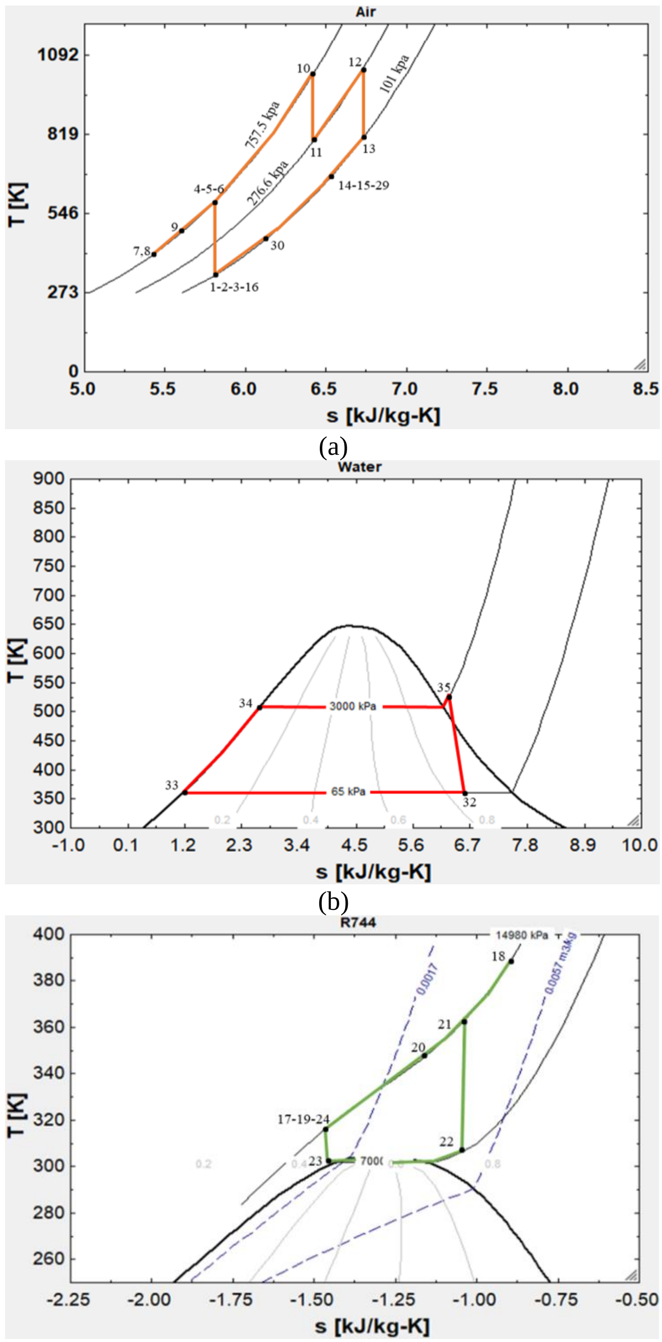

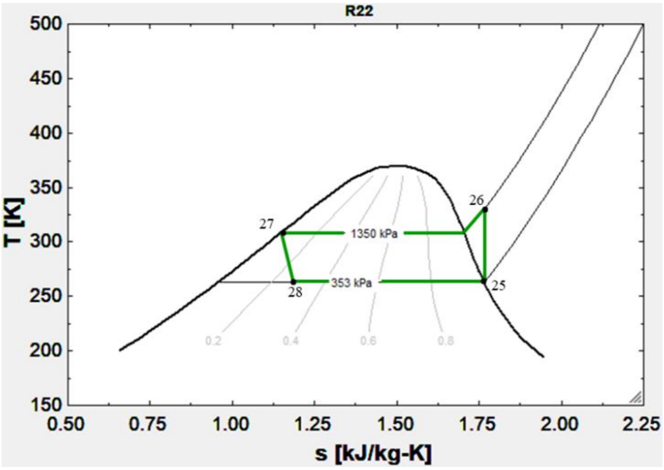

(d)

Figure 5. *T–S* diagram of each sub-cycle: a) Brayton, b) Rankine, c) ORC, and d) Refrigeration

Table 1. The design parameters of employed cycles

Parameter	Unit	Value
Brayton Cycle		
Fluid	----	Air
CR	----	7.5
ε_{Comp}	----	0.85
CEAS volume	m^3	300
ε_{IHE}	----	0.95
ε_{Turb}	----	0.9
Turbine inlet temperature	K	1024
Intercooler efficiency	----	0.95
Heating exchanger efficiency	----	0.95
Solar System		
Direct normal irradiance (DNI)	W/m^2	800
Number of heliostats	----	624
Reflective area of each heliostat	m^2	9.45 × 12.84
Receiver aperture area	m^2	68.1
ε_{Rec}	----	0.95
Rankine Cycle		
Fluid	----	Water
Condenser working pressure	kPa	65
ε_{Pump}	----	0.88
ε_{Turb}	----	0.91
ORC		
Fluid	----	R744
Condenser working pressure	kPa	7000
ε_{Pump}	----	0.86
ε_{Turb}	----	0.95
Refrigeration		
Fluid	----	R22
ε_{Comp}	----	0.90
Evaporator outlet temperature	K	263
Condenser outlet temperature	K	308
Condenser working pressure	kPa	1350
ε_{Eva}	----	0.95
COP	----	4.234
Heating System		
Fluid	----	Water
Inlet water temperature	K	298
Working pressure	kPa	101

To have more details about how the proposed system works, the T-S diagram and the main design parameters of each sub-cycle are presented in Figure 5 and Table 1, respectively.

3. MATHEMATICAL MODELING

For thermodynamically analyzing, each studied component should be considered as a separate control volume. The overall plant is divided into four sub-sections: power generation, refrigerator, heating, and solar systems. Power Generation System (PGS) contains Brayton and Rankine cycles, and the refrigerator is consisted of ORC and compression refrigeration cycle. The following assumption is considered for thermodynamical modeling of proposed system:

-The processes of all devices are assumed as steady-state steady flow (SSSF).

-Kinetic and potential energies and also chemical exergy are negligible.

-The processes of turbines, compressors, and pumps are calculated based on the isentropic efficiency.

The mass and energy conservation and also exergy balance equations in SSSF process for control volume can be written as [3]:

$$\sum\dot{m}_{in} = \sum\dot{m}_{out} \tag{1}$$

$$\dot{Q}_{C.V} - \dot{W}_{C.V} + \sum\dot{m}_{in}h_{in} - \sum\dot{m}_{out}h_{out} = 0 \tag{2}$$

$$\Delta\dot{\psi}_{sys} = \sum\dot{\psi}_{in} - \sum\dot{\psi}_{out} - \dot{\psi}_D \tag{3}$$

where, $\dot{Q}_{C.V}$, $\dot{W}_{C.V}$, $\dot{m}$ and h refer to heat, work, mass flow rates and specific enthalpy in control volume. $\dot{\psi}_{in}$ and $\dot{\psi}_{out}$ present the rate of inlet/outlet transferred exergy by heat, work, and mass, and $\dot{\psi}_D$ is exergy destruction. For the SSSF system, the $\Delta\dot{\psi}_{sys}$ is negligible, so Eq. (3) could be written as [3, 35],

$$\dot{\psi}_Q - \dot{\psi}_W + \dot{\psi}_{mass,in} - \dot{\psi}_{mass,out} = \dot{\psi}_D \tag{4}$$

$$\dot{\psi}_{in} - \dot{\psi}_{out} = h - h_0 - T_0(s - s_0) \tag{5}$$

The solar sub-section contains two parts, namely receiver and heliostat field. The collected worthy heat by the receiver can be computed as [6]:

$$\dot{Q}_{Rec,in} = \eta_{field}.\dot{Q}_{sun} = \eta_{field}.(DNI).A_{hel}.N_{hel} \tag{6}$$

where, η_{field}, DNI, A_{hel} and N_{hel} refer to the efficiency of the heliostat field, direct normal irradiance, the area of concentrating and reflecting sun-beams and the number of heliostats. The heliostat field efficiency can be determined as,

$$\eta_{field} = \eta_{cos}.\eta_{s\&b}.\eta_{int}.\eta_{att}.\eta_{ref} \tag{7}$$

where, η_{cos} refers to cosine effect efficiency; $\eta_{s\&b}$ denotes shading and blocking efficiency; η_{int} presents interception efficiency; η_{att} accounts for the atmospheric attenuation efficiency and η_{ref} is the reflectivity of the heliostats which are considered 0.83, 0.96, 0.97, 0.93 and 0.88, respectively. The used correlation on the first and second law analyzing for each component are summarized in Appendix 1.

To evaluate each section performance based on first and second laws, pure achieved and consumed energies and exergies should be defined, and the rate of achieved to consumed ones are known as first and second laws efficiencies. For example, in PGS section.

$$\dot{W}_{net} = \left(\dot{W}_{GT1} + \dot{W}_{GT2} + \dot{W}_{comp1} + \dot{W}_{comp2}\right)_{Brayton} + \left(\dot{W}_{GTR} + \dot{W}_{PumpR}\right)_{Rankine} \quad (8)$$

$$\eta_I = \frac{\dot{W}_{net}}{\dot{Q}_{IHE}} \quad (9)$$

$$\eta_{II} = \frac{\dot{\psi}_{achieved}}{\dot{\psi}_{consumed}} = \frac{\dot{W}_{net}}{\dot{Q}_{IHE}\left(1 - \frac{T_0}{T_s}\right)} \quad (10)$$

where, T_0 and T_s refer to the ambient and source temperatures near the IHE. The definition of first and second laws efficiencies of each section and overall are reported in Appendix 2.

4. RESULTS AND DISCUSSION

To investigate the proposed system performance, a thermodynamical model of illustrated CCHP system is provided due to the discussed correlations at the previous section in EES commercial software environment. Mass, energy, and exergy equations are applied in each component, and all simplifying assumptions are considered linking employed devices.

4.1 Validation

The proposed cycle is provided by modifying and combining the previous studied subsection and has not examined experimentally, yet. So there is no experimental data for general system. Consequently, to confirm the accuracy of model, each subsystem performance is separately validated using the operating conditions and initial values adopted from references [3, 6]. The maximum errors for output power of different employed components in this study were achieved by less than 0.7, 1.5 and 0.9% for Brayton, Rankine and organic Rankine cycles, respectively. The same range of errors are found for the rest of thermodynamical parameters used in this study, so it can be asserted that the simulator model is reliable and generates valid results.

4.2 General analysis

Thermodynamic properties of each state are presented in Appendix 3. The energy and exergy evaluation of each device, section, and overall for the proposed system could be evaluated adopting the data from Appendix 3. Produced, consumed, and pure power in each section and also the heat transferred in heat exchangers in designed condition are reported in Table 2 and Table 3. From Figure 6 it can be concluded that more than a half proportion of power flow is produced by the turbines which are located in the Brayton cycle while around 30%, 14 MW, is consumed in its two compressors. Net power of Brayton cycle at the designed condition as the main section of PGS is 9.51 MW, 66% of power flow, in which it is increased up to 11.75 MW employing other axillary cycles. ORC driven refrigerator with operation coefficient of 4.23, absorbs 1000 BTU heat from cold ambient employing waste heat of Brayton cycle. By using 1000 MW of Brayton cycle waste heat in the heating system, the overall first law efficiency of proposed CCHP is achieved 55%. However, considering possible improvements of solar section, it should be mentioned that the cost of general performance can be noticeably reduced due to high energy achievement loss in solar tower. The general energy efficiency of proposed system is achieved by 89.2% ignoring the solar tower energy loss, so it can be asserted that the design points of proposed system are sufficiently defined. Furthermore, considering the reported range of energy efficiency (60% to 80%) for the common commercial similar systems [36] it could be asserted that studied CCHP has 9.2% energy saving benefit, may leads less wasted heat (global warming benefits besides less entropy generation). The solar irradiance is a high-quality energy, and enormous irreversibility occurs during the absorption process of this high-temperature energy, about 1125 K, by the receiver. The exergy flow and exergy destruction in each section are shown in Figure 7, and Figure 8 which describe clearly the proportion of solar heat absorbing loss in comparison with the energy loss of other components of general system.

Table 2. The performance of designed CCHP, energy analysis

Parameter	Unit	Value
Compressor 1	MW	6.87
Compressor 2	MW	6.87
Gas turbine	MW	23.25
CAES charge duration	hr	3
CAES discharge duration	hr	5
Rankine turbine	MW	2.24
Rankine pump	kW	6.9
ORC turbine	MW	3.64
ORC pump	kW	2.01
Refrigeration compressor	MW	3.64
Evaporator absorbed heat	MW	6.8
COP	---	4.234
Total energy efficiency	%	55

Table 3. The performance of designed CCHP, energy analysis

Subsystem	Input (MW)	Output (MW)	Destruction (MW)	Exergy Efficiency (%)
Solar tower	63.977	38.386	25.386	61
PGS	38.386	26.270	12.116	68.5
PGS considering solar input	63.977	26.270	37.706	41.1

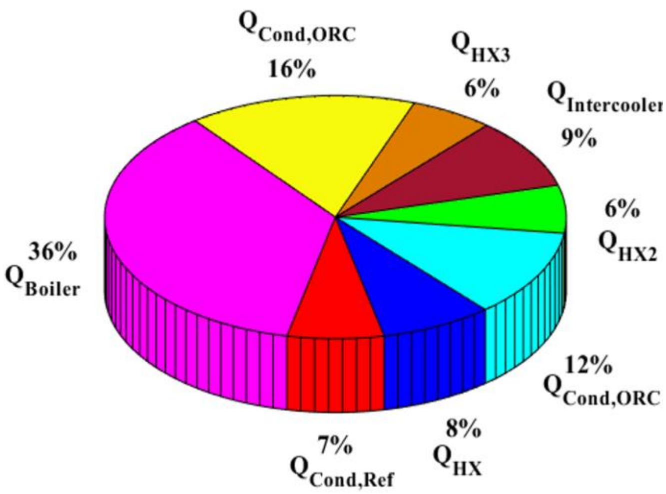

(a)

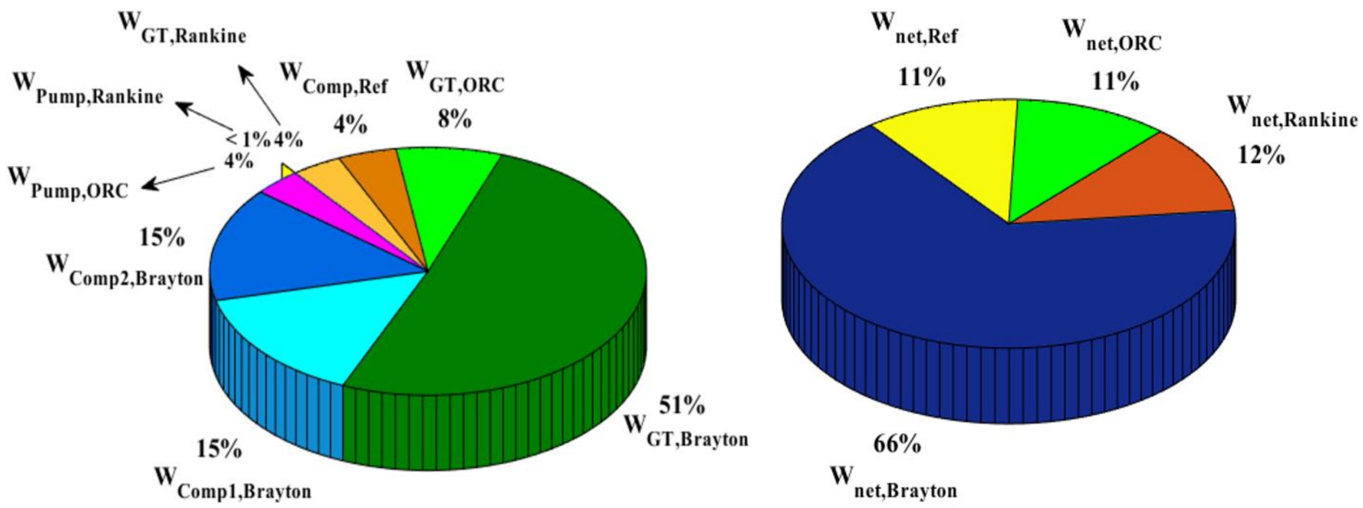

(b) (c)

Figure 6. The proportion of produced/consumed energy: a) Heat transferred by each component, b) Power of each component, c) Pure power of each subsystem

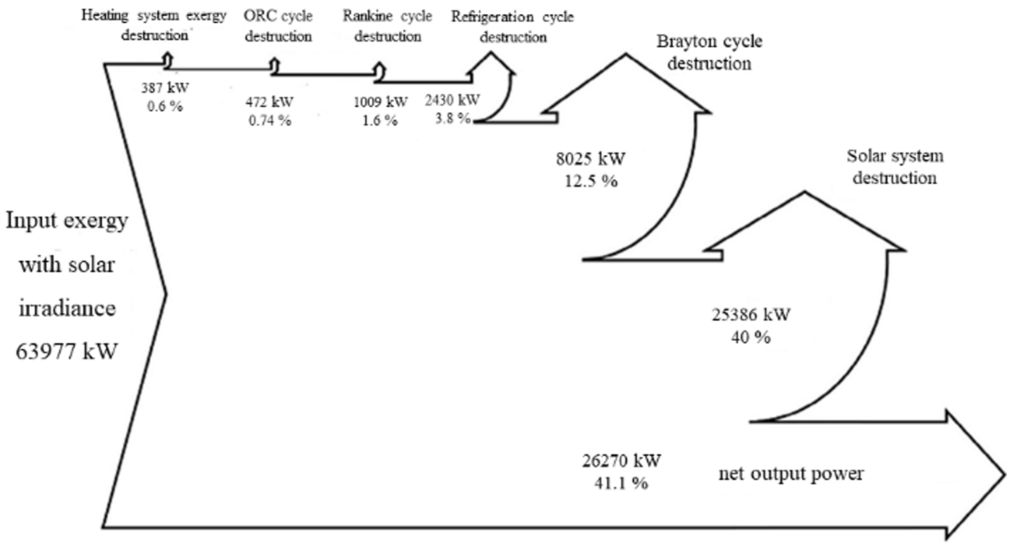

Figure 7. Exergy flow diagram

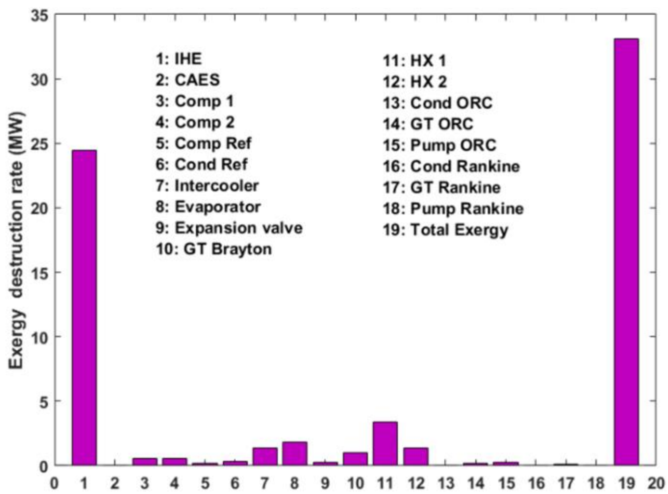

Figure 8. Different sources of exergy destruction

4.3 Parametric study

The parametric studies are generally accomplished to estimate the effects of crucial operating parameters on the overall performance. The effects of compression ratio of Brayton cycle on achieved power and destructed exergy in each section of proposed CCHP is shown in Figure 9. Compressor outflow with higher temperature is attained by increasing the compression ratio. This provides more accessible heat for ORC to drive refrigerator. Therefore, more expansion ratio is feasible in turbines, so generated power in Bryton cycle and also net power generation of PGS were enhanced with compression ratio increment. Due to the Figure 9, net power of PGS, almost doubled by increasing the compression ratio up to 3.5, but the rate of power enhancement is reduced due to the noticeable raise in compressors demanded power. More achieved power from constant inlet energy means less exergy destruction. 2.1 MW destructed exergy reduction in overall system is reported in Figure 9. The variations of energy and exergy efficiencies of each sub-cycle due to compression ratio are shown in Figure 10. The energy efficiency of Brayton cycle as the main core of PGS is increased up to 25% by compression ratio enhancement while due to the particular arrangement of Rankine cycle, its efficiency decreased by 16%. By enhancing both compression and expansion ratios, the temperature of turbine outflow is reduced, so less heat is available for the Rankine cycle and its energy performance is reduced while due to the less temperature gradient in the boiler, its irreversibility is reduced and exergy efficiency is increased by 6.5%.

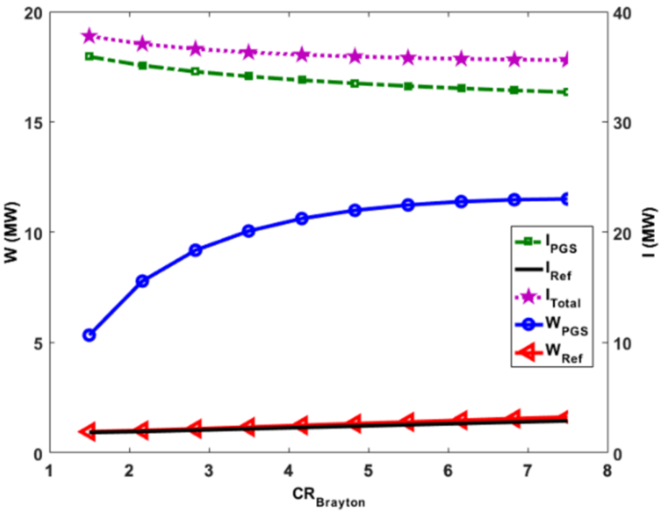

Figure 9. Pure power and exergy destruction variations with compression ratio of Brayton cycle

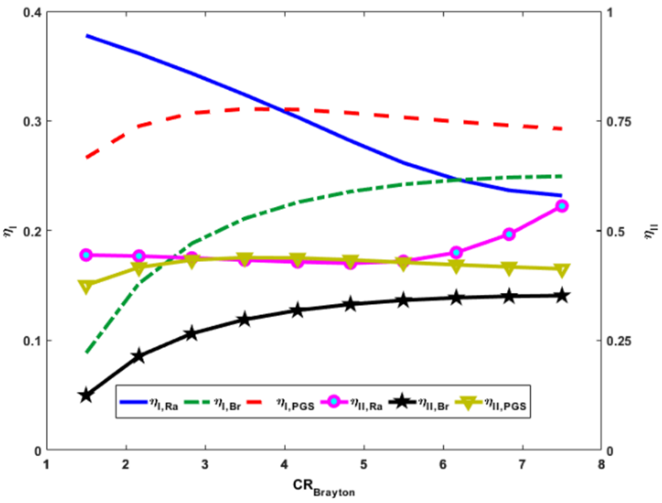

Figure 10. Energy and exergy efficiencies variations with compression ratio of Brayton cycle

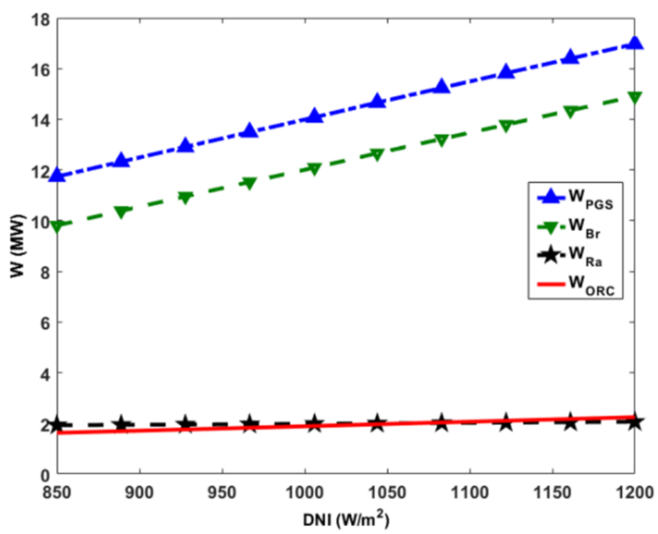

Figure 11. Produced power variations via direct normal irradiance

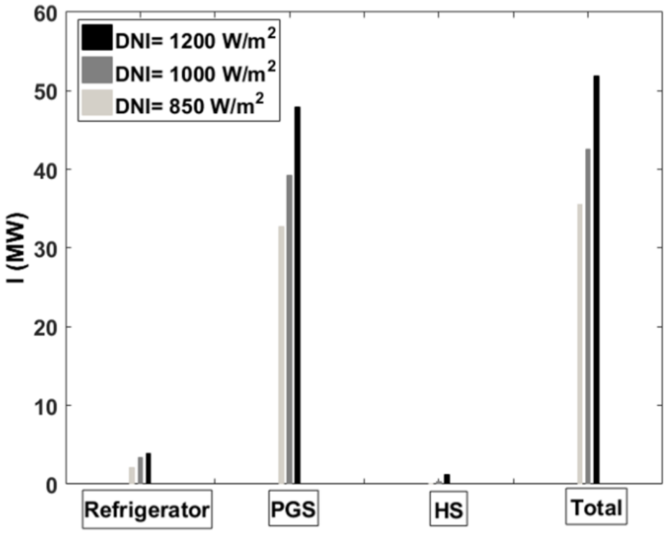

Figure 12. Exergy destruction variations via direct normal irradiance

Direct normal irradiance is the essential parameter of the solar system in which effects directly on inlet and absorbed heat from the sun. It changes during the day time by different factors such as solar angle, sky clearance and etc. However, the main effect of DNI is applied on Brayton cycle. In Figure 11 and Figure 12, it is obviously shown that both generated power and irreversibility of Brayton cycle were increased by 43% and 48%, respectively due to the DNI enhancement between 800 and 1200 W/m^2. This can be the hint for designing more efficient solar heat absorbers.

5. CONCLUSION

In this paper, a solar-driven CCHP system is proposed to achieve higher energy efficiency, and a parametric study on compression ratio, and direct normal irradiance were implemented to estimate the impact of design parameters variations on energy and exergy performance of the proposed system. A CAES technology is utilized in the solar-driven Brayton cycle for running in the peak consumption hours, and a Rankine cycle is employed as an axillary cycle for more power generation. Finally, an ORC driven refrigeration cycle and heating system are considered to convert the waste heat of Brayton cycle to the beneficial energy. The main results were listed below:

- 11.75 MW power, 3.2 MW heating load and 6.8 MW cooling load were provided by the proposed CCHP.
- Designed CCHP is able to run 5 hr in compressor deactivated mode passing peak times.
- Proposed CCHP yields energy efficiency of higher than 89%.
- Using proposed CCHP system brings at least 9% Energy saving in comparison with typical-in-use similar systems.
- Studied CCHP system could be considered more green system than the common ones, having less percent of total entropy generation.
- The most exergy destructor component of the proposed system is solar heat absorber by 72% of general system destructed exergy that could be defined as the target for future study.

REFERENCES

[1] Ahmad, T., Azhar, M., Sinha, M.K., Meraj, M., Mahbubul, I.M., Ahmad, A. (2022). Energy analysis of lithium bromide-water and lithium chloride-water based single effect vapour absorption refrigeration system: A comparison study. Cleaner Engineering and Technology, 7: 100432. https://doi.org/10.1016/j.Clet.2022.100432

[2] Hadi, F.M. (2018). Experimental and theoretical study of the energy flow of a two stages four generators adsorption chiller. Al-Khwarizmi Engineering Journal, 14(2): 129-136. https://doi.org/10.22153/kej.2018.01.002

[3] Balta, M.T., Dincer, I., Hepbasli, A. (2009). Thermodynamic assessment of geothermal energy use in hydrogen production. International Journal of Hydrogen Energy, 34(7): 2925-2939. https://doi.org/10.1016/j.ijhydene.2009.01.087

[4] Eti, S., Yüksel, S., Dinçer, H., Kalkavan, H., Hacioglu, U., Mikhaylov, A., Danish, M.S.S., Pinter, G. (2024). Assessment of technical and financial challenges for renewable energy project alternatives. Cleaner Engineering and Technology, 18: 100719. https://doi.org/10.1016/j.Clet.2023.100719

[5] Rubinetti, D., Iranshahi, K., Onwude, D., Reymond, J., Rajabi, A., Xie, L., Nicolaï, B., Defraeye, T. (2024). Ionic wind amplifier for energy-efficient air propulsion: Prototype design, development, and evaluation. Cleaner Engineering and Technology, 19: 100728. https://doi.org/10.1016/j.Clet.2024.100728

[6] Balta, M.T., Kizilkan, O., Yılmaz, F. (2016). Energy and exergy analyses of integrated hydrogen production system using high temperature steam electrolysis. International Journal of Hydrogen Energy, 41(19): 8032-8041. https://doi.org/10.1016/j.ijhydene.2015.12.211

[7] Haq, H., Valisuo, P., Kumpulainen, L., Tuomi, V. (2020). An economic study of combined heat and power plants in district heat production. Cleaner Engineering and Technology, 1: 100018. https://doi.org/10.1016/j.Clet.2020.100018

[8] Bahari, M., Ahmadi, A., Dashti, R. (2021). Exergo-economic analysis and optimization of a combined solar collector with steam and Organic Rankine Cycle using particle swarm optimization (PSO) algorithm. Cleaner Engineering and Technology, 4: 100221. https://doi.org/10.1016/j.Clet.2021.100221

[9] Khosravi, A., Syri, S., Zhao, X., Assad, M.E.H. (2019). An artificial intelligence approach for thermodynamic modeling of geothermal based-organic Rankine cycle equipped with solar system.Geothermics, 80: 138-154. https://doi.org/10.1016/j.geothermics.2019.03.003

[10] Wang, J., Han, Z., Guan, Z. (2020). Hybrid solar-assisted combined cooling, heating, and power systems: A review. Renewable and Sustainable Energy Reviews, 133: 110256. https://doi.org/10.1016/j.rser.2020.110256

[11] Merchán, R.P., Santos, M.J., Medina, A., Hernández, A. C. (2022). High temperature central tower plants for concentrated solar power: 2021 overview. Renewable and Sustainable Energy Reviews, 155: 111828. https://doi.org/10.1016/j.rser.2021.111828

[12] Papakonstantinou, I., Portnoi, M., Debije, M.G. (2021). The hidden potential of luminescent solar concentrators. Advanced Energy Materials, 11(3): 2002883. https://doi.org/10.1002/aenm.202002883

[13] Samiee, S., Aghdam, A.H. (2024). 4E analysis of a solar, wind and waste heat-driven CCHP system: A case study for a cruise ship. Applied Thermal Engineering, 252: 123600. https://doi.org/10.1016/j.Applthermaleng.2024.123600

[14] Lu, Z., Zhang, H., Duan, L., Wang, Q., Baccioli, A., Desideri, U. (2023). Energy, exergy, environmental and economic performance analysis and optimization of a novel CCHP system integrated with ammonia driven MCFC and solar energy. Energy Conversion and Management, 297: 117751. https://doi.org/10.1016/j.enconman.2023.117751

[15] Assareh, E., Dejdar, A., Ershadi, A., Jafarian, M., et al. (2023). Performance analysis of solar-assisted-geothermal combined cooling, heating, and power (CCHP) systems incorporated with a hydrogen generation subsystem. Journal of Building Engineering, 65: 105727. https://doi.org/10.1016/j.jobe.2022.105727

[16] Liu, J., Li, Y., Meng, X., Wu, J. (2023). Thermodynamic analysis of a novel hybrid fuel cell-combined cooling, heating-and power (CCHP) system-integrated solar-driven biomass gasification for achieving sustainable and efficient poly-generation.International Journal of Green Energy, 20(13): 1524-1544. https://doi.org/10.1080/15435075.2022.2163589

[17] Wang, A., Wang, S., Ebrahimi-Moghadam, A., Farzaneh-Gord, M., Moghadam, A.J. (2022). Techno-economic and techno-environmental assessment and multi-objective optimization of a new CCHP system based on waste heat recovery from regenerative Brayton cycle. Energy, 241: 122521. https://doi.org/10.1016/j.energy.2021.122521

[18] Zare, V., Takleh, H.R. (2020). Novel geothermal driven CCHP systems integrating ejector transcritical CO_2 and Rankine cycles: Thermodynamic modeling and parametric study. Energy Conversion and Management, 205: 112396. https://doi.org/10.1016/j.enconman.2019.112396

[19] Sheykhi, M., Chahartaghi, M., Pirooz, A.A.S., Flay, R.G. (2020). Investigation of the effects of operating parameters of an internal combustion engine on the performance and fuel consumption of a CCHP system. Energy, 211: 119041. https://doi.org/10.1016/j.energy.2020.119041

[20] Bayendang, N.P., Kahn, M.T., Balyan, V. (2023). Combined cold, heat and power (CCHP) systems and fuel cells for CCHP applications: A topological review. Clean Energy, 7(2): 436-491. https://doi.org/10.1093/ce/zkac079

[21] Georgousis, N., Lykas, P., Bellos, E., Tzivanidis, C. (2022). Multi-objective optimization of a solar-driven polygeneration system based on CO_2 working fluid. Energy Conversion and Management, 252: 115136. https://doi.org/10.1016/j.enconman.2021.115136

[22] Zhang, H., Wang, L., Lin, X., Chen, H. (2020). Combined cooling, heating, and power generation performance of pumped thermal electricity storage system based on Brayton cycle. Applied Energy, 278: 115607. https://doi.org/10.1016/j.Apenergy.2020.115607

[23] Cao, Y., Dhahad, H.A., Togun, H., Haghghi, M.A., Athari, H., Mohamed, A.M. (2021). Exergetic and economic assessments and multi-objective optimization of a modified solar-powered CCHP system with thermal

energy storage. Journal of Building Engineering, 43: 102702. https://doi.org/10.1016/j.jobe.2021.102702
[24] Kareem, A.F., Akroot, A., Abdul Wahhab, H.A., Talal, W., Ghazal, R.M., Alfaris, A. (2023). Exergo–economic and parametric analysis of waste heat recovery from taji gas turbines power plant using rankine cycle and organic rankine cycle. Sustainability, 15(12): 9376. https://doi.org/10.3390/su15129376
[25] Lu, M., Du, Y., Yang, C., Zhang, Z., Wang, H., Sun, S. (2024). Performance analysis and multi-objective optimization of a combined system of Brayton cycle and compression energy storage based on supercritical carbon dioxide. Applied Thermal Engineering, 236: 121837. https://doi.org/10.1016/j.Applthermaleng.2023.121837
[26] Farhat, O., Faraj, J., Hachem, F., Castelain, C., Khaled, M. (2022). A recent review on waste heat recovery methodologies and applications: Comprehensive review, critical analysis and potential recommendations. Cleaner Engineering and Technology, 6: 100387. https://doi.org/10.1016/j.Clet.2021.100387
[27] Kumar, A., Rakshit, D. (2021). A critical review on waste heat recovery utilization with special focus on Organic Rankine Cycle applications. Cleaner Engineering and Technology, 5: 100292. https://doi.org/10.1016/j.Clet.2021.100292
[28] Abela, K., Refalo, P., Francalanza, E. (2022). Analysis of pneumatic parameters to identify leakages and faults on the demand side of a compressed air system. Cleaner Engineering and Technology, 6: 100355. https://doi.org/10.1016/j.Clet.2021.100355
[29] Panda, A., Dauda, A.K., Chua, H., Tan, R.R., Aviso, K.B. (2023). Recent advances in the integration of renewable energy sources and storage facilities with hybrid power systems. Cleaner Engineering and Technology, 12: 100598. https://doi.org/10.1016/j.Clet.2023.100598
[30] Mohammadi, A., Ahmadi, M.H., Bidi, M., Joda, F., Valero, A., Uson, S. (2017). Exergy analysis of a combined cooling, heating and power system integrated with wind turbine and compressed air energy storage system. Energy Conversion and Management, 131: 69-78. https://doi.org/10.1016/j.enconman.2016.11.003
[31] Arabkoohsar, A., Dremark-Larsen, M., Lorentzen, R., Andresen, G.B. (2017). Subcooled compressed air energy storage system for coproduction of heat, cooling and electricity. Applied Energy, 205: 602-614. https://doi.org/10.1016/j.Apenergy.2017.08.006
[32] Yang, C., Wang, X., Huang, M., Ding, S., Ma, X. (2017). Design and simulation of gas turbine-based CCHP combined with solar and compressed air energy storage in a hotel building. Energy and Buildings, 153: 412-420. https://doi.org/10.1016/j.enbuild.2017.08.035
[33] Su, B., Han, W., Chen, Y., Wang, Z., Qu, W., Jin, H. (2018). Performance optimization of a solar assisted CCHP based on biogas reforming. Energy Conversion and Management, 171: 604-617. https://doi.org/10.1016/j.enconman.2018.05.098
[34] Eisavi, B., Khalilarya, S., Chitsaz, A., Rosen, M.A. (2018). Thermodynamic analysis of a novel combined cooling, heating and power system driven by solar energy. Applied Thermal Engineering, 129: 1219-1229. https://doi.org/10.1016/j.Applthermaleng.2017.10.132
[35] Jiang, Y., Xu, J., Sun, Y., Wei, C., Wang, J., Liao, S., Ke, D., Li, X., Yang, J., Peng, X. (2018). Coordinated operation of gas-electricity integrated distribution system with multi-CCHP and distributed renewable energy sources. Applied Energy, 211: 237-248. https://doi.org/10.1016/j.Apenergy.2017.10.128
[36] United States Environmenal Protection Agency. (2024). Methods for calculating CHP efficiency. https://www.epa.gov/chp/methods-calculating-chp-efficiency.

NOMENCLATURE

CAES	Compressed Air Energy Storage
CCHP	Combined Cooling Heat and Power
COP	Coefficient of Operation
CV	Control Volume
DNI	Direct Normal Irradiance
GT	Gas Turbine
HS	Heating System
HX	Heat Exchanger
IHE	Intermediate Heat Exchanger
ORC	Organic Rankine Cycle
PGS	Power Generation System
SSSF	Steady State Steady Flow

English symbols

A	Area, m^2
h	Specific enthalpy, kj/kg
I	Irreversibility, kj
m	Mass, kg
N	Number of heliostats
P	Pressure, kPa
Q	Heat Transfer, kj
s	Specific entropy, kj/kgK
T	Temperature, K
W	Work, kj

Greek symbols

ε	Isentropic/Thermal efficiency
η	Efficiency
ρ	Density, kg/m^3
ψ	Exergy, kj

Subscripts

0	Dead state
1	Primary state
2	Final state
comp	Compressor
cond	Condenser
D	Destruction
Eva	Evaporator
hel	Heliostat
IC	Intercooler
in	Inlet
out	Outlet
Ra	Rankine cycle
Rec	Receiver
Ref	Refrigeration cycle
S	Isentropic process
Turb	Turbine

APPENDIX

Appendix 1. Exergy and energy correlations used in system analyzing

Component	Exergy Equation	Energy Equations
Compressor 1	$\dot{\psi}_2 - \dot{W}_{comp1} = \dot{\psi}_4 + \dot{\psi}_{D,comp1}$	$\dot{W}_{comp1} = \dot{m}_2.(h_4 - h_2)$ $\eta_{comp1} = (T_2 - T_{4s})/(T_2 - T_4)$
Compressor 2	$\dot{\psi}_3 - \dot{W}_{comp2} = \dot{\psi}_5 + \dot{\psi}_{D,comp2}$	$\dot{W}_{comp2} = \dot{m}_3.(h_5 - h_3)$ $\eta_{comp2} = (T_3 - T_{5s})/(T_3 - T_5)$
Intercooler	$\dot{\psi}_6 - \dot{\psi}_7 = \dot{\psi}_{18} - \dot{\psi}_{17} + \dot{\psi}_{D,IC}$	$\dot{m}_6.(h_6 - h_7) = \dot{m}_{17}.(h_{18} - h_{17})$
HX 1	$\dot{\psi}_9 - \dot{\psi}_8 = \dot{\psi}_{13} - \dot{\psi}_{14} + \dot{\psi}_{D,HX1}$	$\dot{Q}_{HX1} = \dot{m}_8.(h_9 - h_8) = \dot{m}_{13}.(h_{13} - h_{14})$
IHE	$(\dot{\psi}_{10} - \dot{\psi}_9) + (\dot{\psi}_{12} - \dot{\psi}_{11}) + \dot{\psi}_{D,IHE} = \dot{\psi}_{38} - \dot{\psi}_{39}$	$\dot{Q}_{IHE} = \dot{m}_9.(h_{10} - h_9) + \dot{m}_{11}.(h_{12} - h_{11})$
Heliostat field	$\dot{Q}_{sun}.\left(1 - \frac{T_0}{T_{ref,sun}}\right) = \dot{Q}_{Rec,in}.\left(1 - \frac{T_0}{T_{ref,hel}}\right) + \dot{\psi}_{D,hel}$	$\dot{Q}_{Rec,in} = \eta_{field}.(DNI).A_{hel}.N_{hel}$
Gas turbine 1	$\dot{\psi}_{10} - \dot{W}_{GT1} = \dot{\psi}_{11} + \dot{\psi}_{D,GT1}$	$\dot{W}_{GT1} = \dot{m}_{10}.(h_{10} - h_{11})$ $\eta_{GT1} = (T_{10} - T_{11})/(T_{10} - T_{11s})$
Gas turbine 2	$\dot{\psi}_{12} - \dot{W}_{GT2} = \dot{\psi}_{13} + \dot{\psi}_{D,GT2}$	$\dot{W}_{GT2} = \dot{m}_{12}.(h_{12} - h_{13})$ $\eta_{GT2} = (T_{12} - T_{13})/(T_{12} - T_{13s})$
HX 2	$\dot{\psi}_{15} - \dot{\psi}_{16} = \dot{\psi}_{20} - \dot{\psi}_{19} + \dot{\psi}_{D,HX2}$	$\dot{Q}_{HX2} = \dot{m}_{15}.(h_{15} - h_{16}) = \dot{m}_{19}.(h_{20} - h_{19})$
HX 3	$\dot{\psi}_{29} - \dot{\psi}_{30} = \dot{\psi}_{35} - \dot{\psi}_{34} + \dot{\psi}_{D,HX3}$	$\dot{Q}_{HX3} = \dot{m}_{29}.(h_{29} - h_{30}) = \dot{m}_{34}.(h_{35} - h_{34})$
Rankine turbine	$\dot{\psi}_{35} - \dot{W}_{GTRa} = \dot{\psi}_{32} + \dot{\psi}_{D,GTRa}$	$\dot{W}_{GTRa} = \dot{m}_{35}.(h_{35} - h_{32})$ $\eta_{GTRa} = (T_{35} - T_{32})/(T_{35} - T_{32s})$
Rankine condenser	$\dot{\psi}_{32} - \dot{\psi}_{33} = \dot{\psi}_{D,CondRa}$	$\dot{Q}_{CondRa} = \dot{m}_{32}.(h_{32} - h_{33})$
Rankine pump	$\dot{\psi}_{33} - \dot{W}_{PumpRa} = \dot{\psi}_{34} + \dot{\psi}_{D,PumpRa}$	$\dot{W}_{PumpRa} = \dot{m}_{33}.(h_{34} - h_{33})$ $\eta_{PumpRa} = (T_{33} - T_{34s})/(T_{33} - T_{34})$
HX 4	$\dot{\psi}_{30} - \dot{\psi}_{31} = \dot{\psi}_{37} - \dot{\psi}_{36} + \dot{\psi}_{D,HX4}$	$\dot{Q}_{HX4} = \dot{m}_{30}.(h_{30} - h_{31}) = \dot{m}_{36}.(h_{37} - h_{36})$
ORC turbine	$\dot{\psi}_{21} - \dot{W}_{GTORC} = \dot{\psi}_{22} + \dot{\psi}_{D,GTORC}$	$\dot{W}_{GTORC} = \dot{m}_{21}.(h_{21} - h_{22})$ $\eta_{GTORC} = (T_{21} - T_{22})/(T_{21} - T_{22s})$
ORC condenser	$\dot{\psi}_{22} - \dot{\psi}_{23} = \dot{\psi}_{D,CondORC}$	$\dot{Q}_{CondORC} = \dot{m}_{22}.(h_{22} - h_{23})$
ORC pump	$\dot{\psi}_{23} - \dot{W}_{PumpORC} = \dot{\psi}_{24} + \dot{\psi}_{D,PumpORC}$	$\dot{W}_{PumpORC} = \dot{m}_{23}.(h_{24} - h_{23})$ $\eta_{PumpORC} = (T_{23} - T_{24s})/(T_{23} - T_{24})$
Refrigeration condenser	$\dot{\psi}_{26} - \dot{\psi}_{27} = \dot{\psi}_{D,CondRef}$	$\dot{Q}_{CondRef} = \dot{m}_{26}.(h_{26} - h_{27})$
Refrigeration evaporator	$\dot{\psi}_{25} - \dot{\psi}_{28} = \dot{\psi}_{D,EvaRef}$	$\dot{Q}_{EvaRef} = \dot{m}_{28}.(h_{25} - h_{28})$
Refrigeration compressor	$\dot{\psi}_{25} - \dot{W}_{CompRef} = \dot{\psi}_{26} + \dot{\psi}_{D,CompRef}$	$\dot{W}_{CompRef} = \dot{m}_{25}.(h_{26} - h_{25})$ $\eta_{CompRef} = (T_{26} - T_{25s})/(T_{26} - T_{25})$

Appendix 2. The definition of first and second laws efficiencies for each section

Section	First Law Efficiency / Operation	Second Law Efficiency
Brayton cycle	$\eta_I = \frac{\dot{W}_{net,Br}}{\dot{Q}_{IHE}}$	$\eta_{II} = \frac{\dot{W}_{net,Br}}{\dot{Q}_{IHE}\left(1 - \frac{T_0}{T_s}\right)}$
Rankin cycle	$\eta_I = \frac{\dot{W}_{net,Ra}}{\dot{Q}_{HX_3}}$	$\eta_{II} = \frac{\dot{W}_{net,Ra}}{\dot{Q}_{HX_3}\left(1 - \frac{T_0}{T_s}\right)}$
PGS	$\eta_I = \frac{\dot{W}_{net,Br} + \dot{W}_{net,Ra}}{\dot{Q}_{IHE}}$	$\eta_{II} = \frac{\dot{W}_{net,Br} + \dot{W}_{net,Ra}}{\dot{Q}_{IHE}\left(1 - \frac{T_0}{T_s}\right)}$
ORC	$\eta_I = \frac{\dot{W}_{net,ORC}}{\dot{Q}_{HX_2} + \dot{Q}_{Intercooler}}$	$\eta_{II} = \frac{\dot{W}_{net,ORC}}{\dot{Q}_{HX_2}\left(1 - \frac{T_0}{T_s}\right) + \dot{Q}_{Intercooler}\left(1 - \frac{T_0}{T_s}\right)}$
Refrigerator	$COP = \frac{\dot{Q}_{Eva}}{\dot{W}_{net,ORC}}$	---
Heating system	$\dot{Q}_{HS} = \dot{Q}_{HX_4}$	---
General system	$\eta_I = \frac{\dot{W}_{net,Br} + \dot{W}_{net,Ra} + \dot{Q}_{Eva} + \dot{Q}_{HS}}{\dot{Q}_{IHE}}$	---

Appendix 3. Thermodynamic properties of each state

State	Fluid	P (kPa)	T (K)	s (kj/kg. K)	h (kj/kg)	m (Kg/s)	ψ (kj/kg)
				Compression Train			
1	Air	101	298	5.696	298.4	50	0
2	Air	101	298	5.696	298.4	25	0
3	Air	101	298	5.696	298.4	25	0
4	Air	757.5	567.5	5.773	573.2	25	252
5	Air	757.5	567.5	5.773	573.2	25	252
6	Air	757.5	567.5	5.773	573.2	50	252
				Expansion Train			
7	Air	757.5	320	5.189	320.5	50	173.1
8	Air	757.5	320	5.189	320.5	50	173.1
9	Air	757.5	520	5.682	524	50	229.7
10	Air	757.5	1024	6.417	1074	50	560.8
11	Air	276.6	815.2	6.45	838.9	50	315.9
12	Air	276.6	1025	6.707	1075	50	475
13	Air	101	815.6	6.739	839.4	50	230
14	Air	101	627.2	6.456	636	50	111
15	Air	101	627.2	6.456	636	18.75	111
16	Air	101	298	5.696	298.4	18.75	0
29	Air	101	627.2	6.456	636	31.25	111
30	Air	101	400	5.993	401.3	31.25	14.42
31	Air	101	298	5.696	298.4	31.25	0
				ORC			
17	R744	14980	320.6	-1.427	-200.5	75	225.3
18	R744	14980	379.4	-0.9411	-32.03	75	393.7
19	R744	14980	320.6	-1.427	-200.5	75	225.3
20	R744	14980	345.9	-1.174	-116.1	75	234.2
21	R744	14980	360.4	-1.055	-74.07	150	240.7
22	R744	7000	305.9	-1.051	-98.35	150	215.2
23	R744	7000	301.8	-1.433	-213.9	150	213.6
24	R744	14980	320.6	-1.427	-200.5	150	225.3
				Refrigeration			
25	R22	353	263	1.766	401	43.65	36.35
26	R22	1350	334	1.777	438.4	43.65	70.32
27	R22	1350	308	1.146	243	43.65	63.1
28	R22	353	263	1.165	243	43.65	57.38
				Rankine			
32	Water	65	361.2	6.369	2246	3	353
33	Water	65	361.2	1.17	368.6	3	24.58
34	Water	3000	361.4	1.171	372	3	27.69
35	Water	3000	511.1	6.212	2817	3	970.1
				HS			
36	Water	101	298	0.3648	104.2	10	0
37	Water	101	373.1	1.324	425.6	10	35.43
				Solar System			
38	Air	101	1125	7.363	1513	37.46	717.8
39	Air	101	400	6.534	684.8	37.46	136.6